Title
Crop response functions integrating water, nitrogen, and salinity

Authors
Wang, J
Baerenklau, KA

Publication Date
2014-06-01

DOI
10.1016/j.agwat.2014.03.009

Crop Response Functions Integrating Water, Nitrogen, and Salinity

J.Wang[a,*], K.A.Baerenklau[b]

[a]*Department of Economics, University of New Mexico, Albuquerque, NM, 87131*
[b]*Department of Environmental Sciences, University of California, Riverside, CA, 92521*

Abstract

Process-based simulation models are used to generate seasonal crop yield and nitrate leaching datasets for several important crops. The simulated data is then used to estimate novel three-input crop response functions that account for the effects of interactions and feedback mechanisms in the whole plant-water-nitrogen-salinity system. Comparisons with available field data show that this appears to be a reliable approach for estimating analytical crop response functions with water, nitrogen, and salinity as input factors. Results also demonstrate the shortcomings of using simpler two-input functions. The estimated functions are continuously differentiable and can be easily incorporated into comprehensive agricultural-economic-environmental optimization models, thus facilitating greater utilization of process-based models by a wider range of disciplines.

Keywords: crop response functions, crop yield, nitrate leaching, irrigation, nitrogen, salinity

---

*Corresponding author. Tel.: +1 505 277 2035. E-mail address: wangj@unm.edu (J. Wang).

1. Introduction

Our ability to efficiently manage agricultural water has benefitted in recent years from the development of process-based simulation models that are capable of predicting the effects of varying conditions and management practices on crop yield and the environment. Examples of such models include GLEAMS, EPIC, APSIM, SMCR_N, CropSyst, SWAP, ENVIRO-GRO and HYDRUS (Knisel and Turtola, 2000; Williams et al., 1995; Keating et al., 2003; Zhang et al., 2010; Stöckle et al., 2003; Kroes et al., 2008; Pang and Letey, 1998; Šimůnek et al., 2008). Models such as these typically are based on the specific agronomic and biophysical processes that occur at the plant or plot level in short time steps throughout a growing season, and thus represent our best scientific understanding of those processes.

These models are potentially very useful for researchers in other disciplines who are investigating questions that require accurate representation of agronomic and biophysical processes, possibly at larger spatial and time scales. A prime example is economics which is often concerned with predicting the effects of changes in environmental, economic, or regulatory conditions on grower behavior and welfare, usually at the farm level and over multiple growing seasons. Such predictions invariably require solving a mathematical optimization problem that represents the grower's decision-making process. Although it is possible to link an economic optimization model directly with an external process-based simulation model such that the economic model calls the simulation model each time the optimization routine needs to calculate a level or derivative of one of the simulated variables, this is uncommon in practice due to the requisite programming skills and the substantial computational burden. A recent example of this approach is Lehmann et al. (2013) in which a genetic algorithm is used to bridge the models. Although the authors acknowledge that "the full potential of [process-based] models is only tapped when as many different management variables as possible are considered simultaneously" (p.56), they must limit their choice set to twelve discrete decision variables in order to achieve reasonable computation times. While a decision set of this dimension may be adequate for some single period problems, notwithstanding the lack of continuous choice variables, multi-period problems can easily involve hundreds of decision variables (e.g. Baerenklau et al., 2008).

A far more common approach that is more widely accessible, more computationally feasible, and allows for a richer set of decision variables is to embed in the economic model analytical functions that have been fitted to data generated either from field experiments or by the external simulation model. This amounts to an indirect linkage of the models via the analytical functions, as shown in Figure 1. A recent example of this approach is Finger (2012) who uses simulated yield data from CropSyst to estimate production functions that are then used to predict changes in water and fertilizer application rates by corn producers in response to changing economic conditions. In general terms, such crop response functions relate output variables (e.g., crop yield, pollutant emissions) to the quantity and/or quality of at least one input factor. Crop yield functions have a long history, likely dating back to von Liebig's "law of the minimum" in the mid-1800's, and continue to play an important role in economic analysis of agricultural production (Hexem et al., 1978; Lanzer and Paris, 1981; Letey and Dinar, 1986; Griffin et al., 1987; Berck and Helfand, 1990; Tembo et al., 2008). Tembo et al. (2008) provides an overview. Common applications include yield response to water, salinity, fertilizer, pesticide, or some combination of these.

As concerns about the effects of agricultural pollution have increased, emission functions have been developed to augment crop yield functions (Tanji et al., 1979; Peralta et al., 1994; Pang and Letey, 1998; Knapp and Schwabe, 2008). With both yield and emission functions in hand, economic analysis can be extended to include not only market inputs and outputs but also the nonmarket effects of agricultural production on natural resources and environmental quality. In the case of nitrogen fertilizer, nitrate leaching typically is estimated as a function of applied water and applied nitrogen. When the response functions are embedded in an economic optimization model, the effects of a fertilizer tax, for example, can be estimated on irrigation water use, fertilizer use, crop yield, farm income, nitrate leaching, and ultimately groundwater quality.

Standard practice for empirical specification of such agri-environmental crop response functions has converged on two-input models, typically either water and salinity, or water and nutrients (as in Finger, 2012), or water and pesticides depending on the desired application.[1] Incorporating multiple inputs allows modeling of potentially important interaction effects on crop yield and pollutant emissions. For example, applied irrigation water

[1]Here we refer to the variable inputs for which decisions must be made throughout a growing season. Many other choices by a producer affect yield and emissions, such as planting, harvest, and irrigation technologies. However standard practice is to treat these as fixed factors of production and to estimate crop response functions conditionally on these choices.

is at least as important as applied nitrogen for determining nitrate leaching because water is the main transport medium for dissolved salts (Pang and Letey, 1998). Therefore, in areas where nitrate pollution is a potential threat to public health and the environment, proper evaluation of pollution control policies requires information on the response of both crop yield and nitrate leaching to both water and nitrogen. Another example is the effect of saline irrigation water on nitrate leaching. Total leached nitrogen has been shown to increase due to the effects of salinity stress on water and nutrient uptake (e.g., Pang and Letey, 1998; Ramos et al., 2011).

We are not aware of any previously published crop response functions with three input factors, but such functions would be particularly useful for addressing persistent and emerging problems from irrigated agriculture. Therefore the purpose of this study is to develop, demonstrate, and test a methodology for estimating integrated crop response functions with three input factors; and to disseminate the estimated functions for several important crops that use water, nitrogen and salinity as inputs. In order to address the lack of field experimental data that would support estimation of such functions, we utilize simulations. Novel and generally applicable response functions are derived from the simulated data that account for the effects of interactions and feedback mechanisms in the whole plant-water-nitrogen-salinity system.

2. Methodology

2.1. Function Inputs Specification

Most studies estimate models of crop yield and nitrate leaching using *applied* water and nitrogen fertilizer as inputs (e.g., Helfand and House, 1995; Llewelyn and Featherstone, 1997). From an agronomic perspective, it is the combination of management practices like these and pre-existing soil conditions that determine yield and leaching; yet only a few studies include variables such as soil nitrogen stock as an additional input (Vickner et al., 1998; Martínez and Albiac, 2006). Neglecting to account for soil conditions does not necessarily lead to biased estimation results but it does limit the transferability of the response functions to other regions or even to the same field under different conditions. Our crop response functions use available water, available nitrogen, and exposed salinity as inputs and are thus more general and transferrable. Below we show how to navigate between our input variables and those that are more commonly used.

Water that is available for crop uptake includes irrigation (e.g., surface water, groundwater, recycled drainage water), precipitation, and initial water content in soil. Initial water content is relatively small compared to the amount of applied water, and thus can be assumed away from crop available water (Letey and Knapp, 1995). Denoting the remaining water sources as $w_i, i = 1, \ldots, I$ (cm), crop-available water, w (cm), can be specified as the summation shown in equation (1).

$$w = \sum_{i=1}^{I} w_i \tag{1}$$

Crop-available nitrogen includes only inorganic nitrogen, mainly in the forms of ammonium and nitrate. Direct sources include soil, atmospheric deposition, irrigation, and fertilizer. Additionally, the process of mineralization can slowly convert organic nitrogen to ammonium and thus increase crop-available nitrogen. Following Pang and Letey (1998), it is assumed that nitrification is rapid so that all mineral nitrogen is NO_3. Loss of nitrogen includes volatilization when inorganic fertilizers containing urea are applied to the field and denitrification when nitrate-nitrogen in soil is converted to nitrogen gas through microbial processes. Denoting the average seasonal denitrification rate as λ, the volatilization rate of applied inorganic fertilizer as β, and the average seasonal mineralization rate of organic nitrogen as δ, equation (2) specifies crop available nitrogen n (kg/ha) as a function of soil inorganic nitrogen in^{soil} (kg/ha), soil organic nitrogen on^{soil} (kg/ha), applied inorganic fertilizer in^{fl} (kg/ha) and organic fertilizer on^{fl} (kg/ha), water source w_i (cm) and its nitrogen concentration n_i^w (kg/ha-cm), and the seasonal rate of atmospheric nitrogen deposition d (kg/ha). This equation includes the main processes in and above the root zone that can affect the nitrate leaching rate. Therefore our nitrate leaching functions focus on the amount of nitrate leached out of the root zone. Once this information is available, further steps (beyond our analysis) can be taken to incorporate other processes in the unsaturated and saturated zones to simulate downstream nitrate emissions.

$$n = (1-\lambda)\left(in^{soil} + (1-\beta)\, in^{fl} + \delta\left(on^{soil} + on^{fl}\right) + \sum_{i=1}^{I} w_i\, n_i^w + d\right) \quad (2)$$

A few models have been developed for predicting salt concentration of soil solution under intra-seasonal irrigation (Bresler, 1967; Knapp, 1984) and have been applied to studies on saline water irrigation (e.g., Knapp, 1992; Kan et al., 2002; Kan, 2008). Following Knapp (1992) and Kan et al. (2002), we adapt the salt balance model in Knapp (1984) to obtain the seasonal average for crop exposed salinity s (dS/m), as shown in equation (3). Here, ν (cm) is the field capacity for soil moisture, s^{soil} (dS/m) is the salt concentration of soil solution at the beginning of a growing season, w and w_i are defined in equation (1), s_i^w (dS/m) is the salt concentration of water source w_i, and w_{up} (cm) is the amount of water absorbed by crops. Crop exposed salinity equals the total amount of salt in the soil and from irrigation divided by the total amount of water that is not taken up by the crop.

$$s = \frac{\nu\, s^{soil} + \sum_{i=1}^{I} w_i\, s_i^w}{\nu + w - w_{up}} \tag{3}$$

The crop response functions can be summarized as

$$\begin{aligned} w_{up} &= \Psi_{w_{up}}(w, n, s) && (4)\\ n_{up} &= \Psi_{n_{up}}(w, n, s) && (5)\\ ry &= \Psi_{ry}(w, n, s) && (6)\\ nl &= \Psi_{nl}(w, n, s) && (7) \end{aligned}$$

where w, n, and s are defined above; and w_{up} (cm), n_{up} (kg/ha), ry, and nl (kg/ha) are respectively water uptake, nitrogen uptake, relative yield (the ratio of actual yield to maximum attainable yield), and nitrate leaching.

2.2. *Alternative Function Specification*

The crop response functions defined above depend on absolute values of water, nitrogen, and salinity. As Letey and Dinar (1986) point out, for purposes of transferring such relationships among different geographical areas, it is helpful if these inputs can be expressed in relative terms. We can achieve this by specifying local scaling factors and conducting function transformations.

Relative input values are equal to absolute input values divided by scaling factors, which are listed in Table 1. The three critical scaling factors for a crop in a certain region are maximum water uptake (i.e., potential transpiration) w_{up}^* (cm), maximum nitrogen uptake n_{up}^* (kg/ha), and the salinity critical value $\overline{EC}$ (dS/m), each of which depends on climate, soil conditions, and farming practices. Table 2 summarizes the scaling factors for corn, cotton, and small grains in our study region. These scaling factors can be derived for other regions of interest, and once this information is available, the functions we develop here are transferable to those regions.

Take the relative yield function as an example. We can transform the relative yield function in equation (6) by using an appropriate set of scaling factors to get equation (8), a new function Ω_{ry} that only relies on relative input values. Since local climate conditions, soil conditions, and farming practices are incorporated into local values of w_{up}^*, n_{up}^*, and $\overline{EC}$, this function is independent of these characteristics. The same is true for our water uptake, nitrogen uptake, and nitrate leaching functions when they are expressed similarly in relative terms.

$$
\begin{aligned}
ry &= \Psi_{ry}(w, n, s) \\
&= \Psi_{ry}\big(rw \cdot w^*_{up},\; rn \cdot n^*_{up},\; rs \cdot \overline{EC}\big) \\
&= \Omega_{ry}\big(rw, rn, rs \mid w^*_{up}, n^*_{up}, \overline{EC}\big) \qquad (8)
\end{aligned}
$$

3. Data

Data required for estimating our crop response functions include: applied water, applied nitrogen, soil nitrogen, soil salinity, crop water uptake, crop nutrient uptake, crop yield, and nitrate leaching. We are not aware of any field experiments that have generated a full set of data that could be used to simultaneously estimate the effects water, nitrogen and salinity on yield and leaching. This generally limited availability of field data is likely due to the high cost of experimentally quantifying the combined effects of multiple input factors on yield and solute leaching. This motivates our use of simulation models to generate the required data and our subsequent use of available field data to validate the approach.

3.1. Model selection

Many models have been developed to simultaneously deal with plant growth, water flow, and solute movement at the field level. Among those models, CropSyst, SWAP, ENVIRO-GRO, and HYDRUS contain salinity modules. The four models are similar in terms of their simulation capabilities and each has had its individual modules successfully tested under various empirical conditions (e.g., Pang and Letey, 1998; Stöckle et al., 2003;

Zhang et al., 2010; Bonfante et al., 2010). However, there are few evaluations of these models that simultaneously test both nutrient and salinity modules. One exception is a study by Pang and Letey (1998) that evaluates ENVIRO-GRO against field experiment data and demonstrates good agreement. ENVIRO-GRO might have been an ideal model for the purpose of this study, but the nitrogen module was subsequently modified and is no longer valid (J. Letey, personal communication). Another exception is a recent study by Ramos et al. (2011) that evaluates HYDRUS-1D using data from a field experiment in which corn is irrigated with water of varying nitrogen and salt concentrations. HYDRUS-1D is a software modeling environment for analysis of water flow and solute transport in variably saturated porous media (Šimůnek et al., 2008). It is used worldwide and has been shown to be reliable for modeling water flow and solute transport, especially for processes in soil and groundwater. The results in Ramos et al. (2011) show HYDRUS-1D to be an effective tool for simulating concentrations of both salinity and nitrogen species in soil, and thus we elect to use it here for datast generation.

Ramos et al. (2011) do not utilize the active mechanism of root nutrient uptake in HYDRUS-1D, which is reasonable given their objective to simulate field conditions in a relatively simple way and to provide indicative values. Given our objective of quantifying crop yield and solute leaching, we need to include both active and passive root nitrogen uptake. We simulate the transport of two solutes (salt and nitrogen) in HYDRUS-1D. For salts we assume that there is no uptake by plant roots, while for nitrogen we utilize the compensated root water and nutrient uptake modules through both passive and active mechanisms (as described in Šimůnek and Hopmans (2009)).

Simulation of active solute uptake with multiple solutes is a standard feature of the latest version of HYDRUS-1D.

The outputs from HYDRUS-1D include estimated water uptake, solute uptake, and solute leaching but not crop yield. External functions thus are required to convert water and nutrients uptake from HYDRUS-1D into crop yield. Following Pang and Letey (1998), relative yield is specified as a function of relative water uptake and relative nitrogen uptake:

$$ry = \min\left[ry_w, ry_n\right] = \min\left[\frac{w_{up}}{w^*_{up}}, \Phi\left(\frac{n_{up}}{n^*_{up}}\right)\right] \tag{9}$$

Here Φ represents a quadratic relationship (Pang and Letey, 1998; Feng et al., 2005). Combining HYDRUS-1D outputs with the agronomic model in equation (9) allows us to generate a full set of estimates for crop water uptake, nitrogen uptake, nitrate leaching, and crop yield.

3.2. Validation of Simulated Data

To our knowledge, the best available field experiment data for validating this study are from a corn trial in Davis, California from 1973 to 1976 (Tanji et al., 1979). The field was treated with a wide range of water and nitrogen applications: four different rates of nitrogen fertilizer (0, 90, 180, and 360 kgN/ha) and three different irrigation regimes (20, 60, and 100 cm), with each replicated four times. In addition, nitrogen in harvested grain and stover (i.e., nitrogen uptake) was accurately measured. See Tanji et al. (1979) and Broadbent and Carlton (1980) for detailed descriptions. This high quality dataset has been used previously for model validation (e.g., Tanji et al., 1979; Pang and Letey, 1998, 2000) and continues to be used in more recent work (e.g. Knapp and Schwabe, 2008).

Broadbent and Carlton (1980) report that the Davis corn field trial was established on Yolo fine sandy loam (alluvial, Typic Xerorthent). Therefore in the water flow module of HYDRUS-1D we select sandy loam under the soil catalog, which gives soil hydraulic parameters for typical soil types. The soil bulk density is assumed to be 1.40 Mg/m3 (Pang and Letey, 1998). The longitudinal dispersivity is assumed to be 20 cm and the molecular diffusion coefficient of nitrates and salts in free water is set to zero because the fluxes by diffusion are negligible compared to dispersive transport (Appendix H, Chang et al., 2005). Tanji et al. (1979) also report the maximum root depth for corn in the Yolo soil to be around 2.4 m so we use this value in the root growth module, where the logistic growth function is used to simulate root growth. The root growth factor is specified as 50% after half of the growing season. Because the field trial used nonsaline irrigation water and all plots received pre-irrigation prior to planting, initial soil salinity is assumed to be 0.01 dS/m for all simulations.

Results are presented in Figures 2 and 3. Linear regression equations are reported along with the coefficients of determination. Figure 2 displays field measured nitrogen uptake versus the simulated nitrogen uptake from the model of Tanji et al. (1979) and from HYDRUS-1D. The HYDRUS-1D model shows overall better performance than the widely used Tanji model. The slope coefficient is closer to one and the intercept term is closer to zero and quite small relative to the range of nitrogen uptake magnitudes. The null hypotheses that these coefficients are respectively equal to one and zero cannot be rejected at 95% confidence levels. Figure 3 compares field measured relative yield to the simulated relative yield calculated from equation (9). Although the fit is not as good as that for nitrogen uptake, it is still quite good given the complexities and uncertainties associated with the whole plant-water-nitrogen-salinity system. The simulation results also compare favorably against the results reported by Pang and Letey (1998) in a test of the ENVIRO-GRO model against the same data, where the slope, intercept, and R^2 for nitrogen uptake and relative yield are respectively [0.87, 22.55, 0.75] and [0.85, 0.05, 0.84]. Experimental data on nitrate leaching are not available from the Davis trial so we cannot conduct a similar comparison for our simulated leaching results. However Ramos et al. (2011) demonstrate that HYDRUS-1D can accurately simulate soil water nitrate concentrations in a similar empirical setting. Overall these results suggest that our approach can be used to model nitrogen uptake and relative yield with acceptable levels of accuracy.

3.3. Linearization of Nitrogen Uptake Curves

Inputs for our HYDRUS-1D simulation include raw data on crops (e.g., transpiration rate, salt tolerance, maximum root depth, maximum nitrogen uptake, and maximum water uptake) and soil (e.g., evaporation rate, hydraulic properties, and solute transport parameters).[2] We also must provide crop-specific uptake curves (daily potential uptake) for both water and nitrogen. Most of this information can be obtained locally through either direct

[2]Climate data (e.g., precipitation and average daily temperature) can be input directly into simulation models, or it can be incorporated indirectly through other variable inputs. We have shown in the previous section why the latter is a better approach for improving the transferability of crop response functions.

field measurement or indirect estimation methods. However there is little information on nitrogen uptake curves for crops other than the small grain forages that are discussed in Crohn et al. (2009). To bridge this gap, we use the available data on small grain forages to test the possibility of approximating nitrogen uptake curves with a linear relationship that can be extended to a wider range of crops under the assumption that those uptake curves are approximately linear, as well.

Figure 4 depicts the nitrogen uptake curves for eight small grain forages commonly grown in California in the winter months. These curves are based on the logistic function developed by Crohn et al. (2009), where the nitrogen content of a crop is a function of cumulative growing degree-days (GDD, or thermal time). For ease of comparison, and consistent with the literature (Crohn et al. (2009)), all curves in Figure 4 terminate with the maximum nitrogen uptake $n_{up}^{*} = 250$ kgN/ha and the harvest thermal time $d_{harvest} = 2500$ GDD, which are common values for small grain crops in the San Joaquin Valley of California. In practice, the nitrogen uptake of a crop might be higher than the crop's nitrogen content, since some nitrogen can be lost to the atmosphere. Here we assume that the nitrogen uptake and the nitrogen content of a crop are identical. The curves fall into two categories: exponential for two ryegrass crops and sigmoid for the other crops. As Crohn et al. (2009) point out, the exponential curves are most likely due to forage quality and harvest schedule constraints. Sigmoid curves are widely recognized and applied.

In order to investigate whether the shape of a nitrogen uptake curve significantly affects estimated total nitrogen uptake and relative yield, simulations of Swan oat (top curve in Figure 4), Longhorn oat (middle curve in Figure 4), and Bartali Italian ryegrass (bottom curve in Figure 4) with nonlinear uptake curves are compared to simulations for the same crops with linear uptake curves. For each crop, we specify combinations of five levels of available water ($[0.25, 0.5, 1, 1.5, 2] \times w^*_{up}$), five levels of available nitrogen ($[0.25, 0.5, 1, 1.5, 2] \times n^*_{up}$), and five levels of exposed salinity ($[0, 0.25, 0.5, 0.75, 1] \times \overline{EC}$), which produces 125 input scenarios for each crop. $\overline{EC}$ is the critical value of soil salinity at which crop yield decreases to zero. It is calculated from the salt tolerance parameters of the crop following the approach in Maas and Hoffman (1977). The linear nitrogen uptake curve of a crop is constructed from the crop's maximum nitrogen uptake, the harvest thermal time, and the cumulative thermal time over the season d (GDD), as shown in equation (10). All other HYDRUS-1D specifications are held constant for each pair of simulations.

$$n^d_{up} = \frac{n^*_{up}}{d_{harvest}} d \tag{10}$$

Figure 5 displays a comparison of the simulation results. Most results closely track the 45-degree line implying little discernible effect of linearizing the nitrogen uptake curve. The points that visibly lie off the 45-degree line are scenarios in which crops receive sufficient water with low salinity but little nitrogen, which rarely happens in practice. The t-statistics for the three relationships (not shown) suggest that the relative yields of Longhorn oat and Bartali Italian ryegrass are not statistically different from their linearized versions at the 95% level; the relative yield of Swan Oat is statistically different from its linearized version at the 95% level due to a very small standard error on the slope coefficient, but the difference is not practically significant (about 1.3% of the estimated yield). We conclude that any nonlinear terms in a nitrogen uptake curve can be safely disregarded for our purposes, and thus adopt the linear relationship in equation (10) that can be applied to any crop for which an estimate of the maximum nitrogen uptake is available.

4. Results

We estimate the crop response functions in equations (4)-(7) for corn, cotton, and winter small grains using simulated datasets. For each crop, we specify combinations of at least five levels of available water ($[0.25,\ 0.5, 1, 1.5, 2] \times w^*_{up}$), five levels of available nitrogen ($[0.25, 0.5, 1, 1.5, 2] \times n^*_{up}$), and six levels of exposed salinity ($[0, 0.2, 0.4, 0.6, 0.8, 1] \times \overline{EC}$), which produces at least 150 input scenarios for each crop. Some of these input values may seem extreme, but they are selected in order to cover most, if not all, of a producer's possible operating scenarios, including potentially stringent environmental regulations. The highest level of available water is double the maximum water uptake, taking into account that the operator might apply excess water to flush salts out of the root zone. The highest level of available nitrogen is also double the maximum nitrogen uptake, since both animal waste and commercial fertilizers tend to be over-applied to crop fields. And exposed salinity covers the entire range in which it is possible for a crop to grow.

For each combination of input values, we use HYDRUS-1D and the agronomic model in equation (9) to simulate water uptake, nitrogen uptake, relative yield, and nitrate leaching. We then use this data to estimate crop response and nitrate leaching as smooth functions of the input values. Drainage water and salt leaching are beyond the scope of this paper but can be calculated using mass balance relationships (see (Knapp and Baerenklau, 2006)).

The forms of the water and nitrogen uptake and relative yield functions are developed from the traditional Mitscherlich-Baule functional form, which is discussed below. Because the estimation methods for these three functions are similar, we only present the procedure for estimating the crop relative yield function in the following section. The nitrate leaching function is adapted from Knapp and Schwabe (2008). We use corn as an example to illustrate the whole estimation procedure.

4.1. Relative Yield Function

Various forms have been proposed for crop yield functions. Griffin et al. (1987) provide a thorough review of twenty traditional and popular functional forms. They also discuss guidelines for form selection, one of which pertains to application-specific characteristics. Since we expect the resulting functions in this paper to be incorporated into economic optimization models, continuous differentiability is a desirable property. Llewelyn and Featherstone (1997) compare five functional forms using corn yield data from the CERES-Maize simulator for western Kansas. Corn yield is estimated as a function of nitrogen and irrigation water. Their results favor the Mitscherlich-Baule (MB) form over all other specifications. Shenker et al. (2003) measure the yield response of sweet corn to the combined effects of nitrogen fertilization and water salinity over a wide range of nitrogen and salinity levels. Two functional forms (Liebig–Sprengel and MB) are evaluated based on the measured data. The results suggest that either functional form can successfully predict water needs, nitrogen needs, and yield. Liebig–Sprengel is a minimization function derived from von Liebig's "law of the minimum". It results in a step-wise response curve that is not differentiable. Therefore, MB is chosen as the base functional form for crop relative yield in this study. We also compare our MB function with quadratic and square root functions of corn using pair-wise P-tests, as used in Frank et al. (1990) and Llewelyn and Featherstone (1997). The MB function is found to be favored over the other functional forms.

The traditional MB function is usually expressed as equation (11), where a calibrates the upper limit on yield and the b_i are parameters for the input factors X_i. This function exhibits continuously positive marginal productivities of input factors and allows for factor substitution.

$$Y = a \prod_i \left[1 - e^{-b_i^1\left(X_i + b_i^0\right)}\right] \tag{11}$$

Either absolute yield or relative yield can be the dependent variable, with a equal to the maximum attainable yield when estimating the absolute yield and equal to one when estimating the relative yield. Using this form, relative yield as a function of three inputs can be written as equation (12), where $b_w, b_{n,}$ and b_s are parameters for crop available water, available nitrogen, and exposed salinity.

$$\begin{aligned} ry &= \Psi_{ry}\left(w, n, s\right) \\ &= \left[1 - e^{-b_w^1\left(w - b_w^0\right)}\right]\left[1 - e^{-b_n^1\left(n - b_n^0\right)}\right]\left[1 - e^{-b_s^1\left(s - b_s^0\right)}\right] \end{aligned} \tag{12}$$

Our efforts to estimate equation (12) directly from the simulated data did not produce good results. Inspection of the simulated data for each salinity level revealed that relative yield is roughly "bell shaped" in the water dimension. We thus modify the water parameter in equation (12) so that it, too, is bell shaped. To do this, we use a parameterized variant of the logistic probability density function (preferred over the normal distribution because of its heavier tails) and define it as the water coefficient φ shown in equations (13) and (14).[3] For each salinity level, the crop relative yield function is then defined as

$$\begin{aligned} ry &= \psi_{ry}\left(w, n \mid s\right) \\ &= \left[1 - e^{-b_w^1\left(\varphi(w)\,w - b_w^0\right)}\right]\left[1 - e^{-b_n^1\left(n - b_n^0\right)}\right] \end{aligned} \tag{13}$$

where

$$\varphi\left(w\right) = \frac{4e^{d_1 w + d_0}}{\left(1 + e^{d_1 w + d_0}\right)^2} + d_2 \tag{14}$$

As shown in Figure 6, this approach produces very good results ($R^2 > 0.99$ for each salinity level). However it produces a set of coefficient estimates $\boldsymbol{\Upsilon} \equiv \{b_w^1, b_w^0, b_n^1, b_n^0, d_0, d_1, d_2\}$ and thus a yield function that is specific to each simulated salinity level. To get a single continuously differentiable yield function that operates over all water, nitrogen, and salinity levels, we note that each coefficient estimate is effectively a function of salinity so we proceed to estimate a parametric function of salinity for each coefficient. Salinity thus

[3] The coefficient 4 is applied to approximately standardize the range of the function to the $[0, 1]$ interval.

enters the yield function indirectly through its influence on the water and nitrogen parameters rather than directly as a separate multiplicative term.

This approach also reduces the computational requirement by breaking down the problem into two subproblems. First, estimate equation (13) once for each value of $s = [0, 0.2, 0.4, 0.6, 0.8, 1] \times \overline{EC}$, each time using the subset of simulated data points that corresponds to the selected salinity value. These estimations produce the surfaces shown in Figure 6 for the case of corn. As noted by Griffin et al. (1987), convergence problems may arise when estimating the (modified) MB functions during the first step of this procedure. We found that standard methods were sufficient for overcoming such difficulties. These include: (1) increasing iteration limits for the regression models, (2) specifying alternative starting values for the parameters, and (3) using data visualization as a complementary method for goodness-of-fit assessment (e.g., Figures 6 and 9). Second, estimate each parameter $\Upsilon_i \in \boldsymbol{\Upsilon}$ as a polynomial function of salinity using the coefficient estimates from the first subproblem as data. Figure 7 depicts the regression curves for the case of corn. Again, agreement between the data and functions is generally very good. Finally, substitute the fitted polynomial equations into equations (13) and (14) to get the crop relative yield function with three input variables, as shown in equation (15). For the case of corn, this approach is verified by the excellent agreement between the simulated data and the fitted relative yield shown in Figure 8.

$$
\begin{aligned}
ry &= \Psi_{ry}\left(w,n,s\right) \\
&= \left[1-e^{-b_w^1(s)\left(\varphi(w|d_0(s),d_1(s),d_2(s))\,w-b_w^0(s)\right)}\right]\left[1-e^{-b_n^1(s)\left(n-b_n^0(s)\right)}\right] \qquad (15)
\end{aligned}
$$

Table 3 summarizes the parameter estimates for the corn relative yield function. Each row shows the coefficients that specify each parameter $\Upsilon_i \in \boldsymbol{\Upsilon}$ as a polynomial function of salinity, as well as the R^2 values for each polynomial regression. The last column shows the R^2 value for a linear regression of the estimated relative yield from equation (15) versus the simulated data. As can be seen in the table, the R^2 values are generally very good. Similary, Tables 4 and 5 summarize the parameter estimates for the corn water uptake function and nitrogen uptake function.

4.2. Nitrate Leaching Function

We use the same comparison tests as for the crop relative yield function to compare four forms of nitrate leaching functions (test results available upon request). A function adapted from Knapp and Schwabe (2008) outperforms the quadratic, cubic, and square root functions, mainly because of its convex-concave properties and guarantee of a plateau maximum. In Knapp and Schwabe (2008), nitrate leaching is specified as a function of soil nitrogen, applied nitrogen, infiltrated water, and a set of estimable parameters. Equation (16) shows their function with our notation.

$$
nl = \psi_{nl}\left(w,n \mid s\right) = \frac{\vartheta_n \cdot n}{1+e^{-\vartheta_w^1\left(w-\vartheta_w^0\right)}} \qquad (16)
$$

Salinity is notably absent from this leaching equation. Thus the parameter vector $\boldsymbol{\vartheta} \equiv \{\vartheta_w^1, \vartheta_w^0, \vartheta_n\}$ implicitly applies to a fixed salinity level. To incorporate varying salinity levels, we again specify parameters as functions of salinity levels as in the crop relative yield functions. Our nitrate leaching function with three input factors is specified in equation (17).

$$nl = \Psi_{nl}\left(w, n, s\right) = \frac{\vartheta_n(s) \cdot n}{1 + e^{-\vartheta_w^1(s)(w - \vartheta_w^0(s))}} \tag{17}$$

Here we adopt the same estimation procedure as for the crop relative yield functions. For the case of corn, first estimate equation (16) for each value of $s = 0, 6, 12, 18, 24, 30$ dS/m to get the surfaces shown in Figure 9. Second, estimate each parameter $\vartheta_i \in \boldsymbol{\vartheta}$ as a polynomial function of salinity. Figure 10 depicts the regression curves. Finally, substitute the fitted polynomial equations into equation (16) to get the nitrate leaching function with three input variables, as shown in equation (17). Figure 11 demonstrates that the estimated nitrate leaching function fits the simulated data very well for the case of corn.

Table 6 summarizes the parameter estimates for the corn nitrate leaching function. Each row shows the coefficients that specify each parameter $\vartheta_i \in \boldsymbol{\vartheta}$ as a polynomial function of salinity, as well as the R^2 values for each polynomial regression. The last column shows the R^2 value for a linear regression of the estimated nitrate leaching from equation (17) versus the simulated data. As in Table 3, the R^2 values are again very good. We follow the same procedure to estimate the response functions (water uptake, nitrogen uptake, relative yield, and nitrate leaching) for cotton and small grains. The estimation results are reported in Tables 7 and 8.

5. Discussions

The datasets we use for estimating our crop response functions are simulated from a hydrologic model consisting of water flow, solute transport, and root growth modules, in conjunction with a simple but effective analytical agronomic model. Therefore, our crop response functions are able to account for the effects of interactions and feedback mechanisms in the whole plant-water-nitrogen-salinity system. Figures 12 and 13 present two examples illustrating the importance of using these integrated crop response functions as opposed to a traditional function with only two inputs.

Figure 12 demonstrates the relationship between corn relative yield and available water under three different salinity levels (0.2, 2, and 10 dS/m), given a fixed level of available nitrogen (200 kg/ha). For each salinity level, the relative yield gradually increases to a plateau and then declines. This is consistent with the findings in Pang and Letey (1998) and Knapp and Schwabe (2008). With fixed nitrogen and excessive water, more nitrate is leached out of the root zone and thus less nitrogen is available for crop uptake. Moreover the figure demonstrates the significant effect of salinity on yield that would otherwise be omitted from a standard two-input (water and nitrogen) crop response model.

Figure 13 demonstrates the relationship between nitrate leaching and available water under three different salinity levels (0.2, 2, and 10 dS/m), given a fixed level of available nitrogen (200 kg/ha). For each salinity level, nitrate leaching significantly increases when available water exceeds the plant uptake capacity and eventually reaches a plateau. Comparing the three curves shows that high salinity levels tend to generate high nitrate leaching.

The underlying mechanisms are well explained in Pang and Letey (1998): "Salinity leads to reduced plant growth, which leads to reduced evapotranspiration, which leads to more leaching, which leads to salt removal from the root zone. However, the leaching also removes other chemicals such as N and pesticides. Reduced N leads to reduced plant growth, which leads to less evapotranspiration, which leads to more leaching, which leads to even less N in the root zone" (p. 1426). In short, the interactions and feedbacks between plant growth, evapotranspiration, and leaching are complex. Therefore important information can be lost and incorrect nitrate leaching estimates can be generated if common two-input crop response functions are applied in cases where water, nitrogen, and salinity actually interact.

One such case where it is important to account for interactions among all three factors is land-application of animal manure. The consolidation trend in animal agriculture has resulted in waste generation rates that far exceed the ability of crops to utilize waste nutrients as fertilizer (Gollehon et al., 2001). In the absence of regulation, the most cost-effective disposal option for farmers is to over-apply manure to crops, resulting in both groundwater and surface water pollution (Harter et al., 2002). Because animal manure usually contains high concentrations of nutrients and salts, both of which affect crop growth and the ability of crops to uptake nitrogen, evaluations of animal waste management practices and policies should be based on integrated crop response functions that relate crop yield and pollutant emission to water, nitrogen, and salinity. Such an application is demonstrated in Wang and Baerenklau (2014), where the crop response functions developed here are incorporated into a dynamic environmental-economic model for policy analysis. These crop response functions also would be useful more broadly for economic analyses of irrigated agriculture in arid and semi-arid regions where problems of water scarcity, excess nutrients, and high salinity commonly coexist.

6. Conclusions

Integrated models of agri-environmental systems are potentially very useful for evaluating proposed or anticipated changes in operating conditions (e.g., policies, technologies, prices, and climate). The ability to predict both economic and environmental outcomes within these models is crucial for making accurate evaluations. Although process-based simulations models potentially can be linked to economic optimization models in order to address these questions, this approach can be problematic and remains uncommon. Instead, analytical crop response functions have provided the foundation for such evaluations for many years, but have been limited to only one or two input factors largely due to the limited availability of data for estimation.

This article uses a process-based model to generate simulated crop yield and nitrate leaching datasets that are then used to estimate novel three-input crop response functions for several important crops. The functions account for the effects of interactions and feedback mechanisms in the whole plant-water-nitrogen-salinity system, and thus facilitate greater utilization of the knowledge contained in process-based models by other disciplines. Comparisons with available field data show that this appears to be a reliable approach for estimating integrated crop response functions with water, nitrogen, and salinity as input factors. Comparisons with simpler two-input functions demonstrate the shortcomings of those functions, which continue to be widely used in disciplines such as economics.

Because the crop response functions developed here use available water, available nitrogen, and exposed salinity as inputs, they are more general than functions based only on the characteristics of applied inputs. It is straightforward to navigate between our input variables and those that are more commonly used, provided sufficient information about soil characteristics is available. Furthermore we demonstrate how to express our inputs in relative terms to facilitate transfer of our crop response functions across different geographic areas.

Acknowledgement

The authors would like to thank Dr. Jirka Šimůnek of the University of California, Riverside for essential help with HYDRUS; Drs. Keith Knapp, Kurt Schwabe, John Letey, and Ariel Dinar of the University of California, Riverside for helpful comments and suggestions; and Sunny Sohrabian, an undergraduate student at the University of California, Riverside, for help with dataset generation.

References

Baerenklau, K. A., Nergis, N., Schwabe, K. A., 2008. Effects of nutrient restrictions on confined animal facilities: Insights from a structural-dynamic model. Canadian Journal of Agricultural Economics 56 (2), 219–241.

Berck, P., Helfand, G., 1990. Reconciling the von Liebig and differentiable crop production functions. American Journal of Agricultural Economics 72 (4), 985–996.

Bonfante, A., Basile, A., Acutis, M., De Mascellis, R., Manna, P., Perego, A., Terribile, F., 2010. SWAP, CropSyst and MACRO comparison in two contrasting soils cropped with maize in northern Italy. Agricultural water management 97 (7), 1051–1062.

Bresler, E., 1967. A model for tracing salt distribution in the soil profile and estimating the efficient combination of water quality and quantity under varying field conditions. Soil Science 104 (4), 227–233.

Broadbent, F. E., Carlton, A. B., 1980. Methodology for field trials with nitrogen-15-depleted nitrogen. Journal of Environmental Quality 9 (2), 236–242.

Chang, A. C., Harter, T., Letey, J., Meyer, D., Meyer, R. D., Mathews, M. C., Mitloehner, F., Pettygrove, S., Robinson, P., Zhang, R., 2005. Managing dairy manure in the Central Valley of California. Tech. rep.

Crohn, D. M., Mathews, M. C., Putnam, D. H., 2009. Nitrogen content curves for small grain forage crops. Transactions of the ASAE 52 (2), 459–467.

Feng, G. L., Letey, J., Chang, A. C., Campbell-Mathews, M., 2005. Simulating dairy liquid waste management options as a nitrogen source for crops. Agriculture, Ecosystems & Environment 110 (3-4), 219–229.

Finger, R., 2012. Modeling the sensitivity of agricultural water use to price variability and climate change–An application to Swiss maize production. Agricultural Water Management 109, 135–143.

Frank, M. D., Beattie, B. R., Embleton, M. E., 1990. A comparison of alternative crop response models. American Journal of Agricultural Economics 72 (3), 597–603.

Gollehon, N. R., Caswell, M., Ribaudo, M., Kellogg, R. L., Lander, C., Letson, D., 2001. Confined animal production and manure nutrients. Tech. rep., United States Department of Agriculture, Economic Research Service.

Griffin, R. C., Montgomery, J. M., Rister, M. E., 1987. Selecting functional form in production function analysis. Western Journal of Agricultural Economics 12 (2), 216–227.

Harter, T., Meyer, R. D., Mathews, M. C., 2002. Nonpoint source pollution from animal farming in semi-arid regions: Spatio-temporal variability and groundwater monitoring strategies. In: Ribeiro, L. (Ed.), 2002, Future Groundwater Resources at Risk, Proceedings of the 3rd International Conference, Lisbon, Portugal, June 2001. pp. 363–372.

Helfand, G. E., House, B. W., 1995. Regulating nonpoint source pollution under heterogeneous conditions. American Journal of Agricultural Economics 77 (4), 1024–1032.

Hexem, R. W., Heady, E. O., et al., 1978. Water production functions for irrigated agriculture. Iowa State University Press.

Kan, I., 2008. Yield quality and irrigation with saline water under environmental limitations: The case of processing tomatoes in california. Agricultural Economics 38 (1), 57–66.

Kan, I., Schwabe, K. A., Knapp, K. C., 2002. Microeconomics of irrigation with saline water. Journal of Agricultural and Resource Economics 27 (1), 16–39.

Keating, B. A., Carberry, P. S., Hammer, G. L., Probert, M. E., Robertson, M. J., Holzworth, D., Huth, N. I., Hargreaves, J. N., Meinke, H., Hochman, Z., et al., 2003. An overview of APSIM, a model designed for farming systems simulation. European Journal of Agronomy 18 (3), 267–288.

Knapp, K. C., 1984. Steady-state solutions to soil salinity optimization problems. American Journal of Agricultural Economics 66 (3), 279–285.

Knapp, K. C., 1992. Irrigation management and investment under saline, limited drainage conditions: 2. characterization of optimal decision rules. Water Resources Research 28 (12), 3091–3097.

Knapp, K. C., Baerenklau, K. A., 2006. Ground water quantity and quality management: agricultural production and aquifer salinization over long time scales. Journal of Agricultural and Resource Economics 31 (3), 616–641.

Knapp, K. C., Schwabe, K. A., 2008. Spatial dynamics of water and nitrogen management in irrigated agriculture. American Journal of Agricultural Economics 90 (2), 524–539.

Knisel, W. G., Turtola, E., 2000. GLEAMS model application on a heavy clay soil in finland. Agricultural Water Management 43 (3), 285–309.

Kroes, J. G., Van Dam, J. C., Groenendijk, P., Hendriks, R., Jacobs, C.,

2008. SWAP version 3.2: Theory description and user manual. Alterra Wageningen, The Netherlands.

Lanzer, E. A., Paris, Q., 1981. A new analytical framework for the fertilization problem. American Journal of Agricultural Economics 63 (1), 93–103.

Lehmann, N., Finger, R., Klein, T., Calanca, P., Walter, A., 2013. Adapting crop management practices to climate change: Modeling optimal solutions at the field scale. Agricultural Systems 117, 55–65.

Letey, J., Dinar, A., 1986. Simulated crop-water production functions for several crops when irrigated with saline waters. Hilgardia 54 (1), 1–32.

Letey, J., Knapp, K. C., 1995. Simulating saline water management strategies with application to arid-region agroforestry. Journal of Environmental Quality 24 (5), 934–940.

Llewelyn, R. V., Featherstone, A. M., 1997. A comparison of crop production functions using simulated data for irrigated corn in western Kansas. Agricultural Systems 54 (4), 521–538.

Maas, E. V., Hoffman, G. J., 1977. Crop salt tolerance–current assessment. Journal of the Irrigation and Drainage Division 103 (2), 115–134.

Martínez, Y., Albiac, J., 2006. Nitrate pollution control under soil heterogeneity. Land Use Policy 23 (4), 521–532.

Pang, X. P., Letey, J., 1998. Development and evaluation of ENVIRO-GRO, an integrated water, salinity, and nitrogen model. Soil Science Society of America Journal 62 (5), 1418–1427.

Pang, X. P., Letey, J., 2000. Organic farming challenge of timing nitrogen availability to crop nitrogen requirements. Soil Science Society of America Journal 64 (1), 247–253.

Peralta, R. C., Hegazy, M. A., Musharrafieh, G. R., 1994. Preventing pesticide contamination of groundwater while maximizing irrigated crop yield. Water Resources Research 30 (11), 3183–3193.

Ramos, T. B., Šimůnek, J., Gonçalves, M. C., Martins, J. C., Prazeres, A., Castanheira, N. L., Pereira, L. S., 2011. Field evaluation of a multicomponent solute transport model in soils irrigated with saline waters. Journal of Hydrology 407 (1), 129–144.

Shenker, M., Ben-Gal, A., Shani, U., 2003. Sweet corn response to combined nitrogen and salinity environmental stresses. Plant and Soil 256 (1), 139–147.

Šimůnek, J., Hopmans, J. W., 2009. Modeling compensated root water and nutrient uptake. Ecological Modelling 220 (4), 505–521.

Šimůnek, J., van Genuchten, M. T., Šejna, M., 2008. Development and applications of the HYDRUS and STANMOD software packages and related codes. Vadose Zone Journal 7 (2), 587–600.

Stöckle, C. O., Donatelli, M., Nelson, R., 2003. Cropsyst, a cropping systems simulation model. European Journal of Agronomy 18 (3), 289–307.

Tanji, K. K., Broadbent, F. E., Mehran, M., Fried, M., 1979. An extended version of a conceptual model for evaluating annual nitrogen leaching losses from cropland. Journal of Environmental Quality 8 (1), 114–120.

Tembo, G., Brorsen, B. W., Epplin, F. M., Tostão, E., 2008. Crop input response functions with stochastic plateaus. American Journal of Agricultural Economics 90 (2), 424–434.

Vickner, S. S., Hoag, D. L., Frasier, W. M., Ascough, J. C., 1998. A dynamic economic analysis of nitrate leaching in corn production under nonuniform irrigation conditions. American Journal of Agricultural Economics 80 (2), 397–408.

Wang, J., Baerenklau, K. A., 2014. How inefficient are nutrient application limits? A dynamic analysis of groundwater nitrate pollution from CAFOs. University of New Mexico Economics Department Working Paper.Available at https://dl.dropboxusercontent.com/u/17693201/WorkingPapers/cafoPolicyWorkingPaper.pdf.

Williams, J. R., Singh, V., et al., 1995. The EPIC model. Computer Models of Watershed Hydrology, Water Resources Publications, Highlands Ranch.

Zhang, K., Greenwood, D. J., Spracklen, W. P., Rahn, C. R., Hammond, J. P., White, P. J., Burns, I. G., 2010. A universal agro-hydrological model for water and nitrogen cycles in the soil–crop system SMCR_N: Critical update and further validation. Agricultural Water Management 97 (10), 1411–1422.

Table 1: Scaling factors for calculating relative value

Absolute Value	Scale	Relative value
Available water w [cm]	Maximum water uptake w^*_{up} [cm]	$rw = \frac{w}{w^*_{up}}$
Available nitrogen n [kgN/ha]	Maximum nitrogen uptake n^*_{up} [kgN/ha]	$rn = \frac{n}{n^*_{up}}$
Soil salinity s [dS/m]	Salinity critical value $\overline{EC}$ [dS/m]	$rs = \frac{s}{\overline{EC}}$

Table 2: Scaling factors for corn, cotton, and small grains in the study region

Scale	Corn	Cotton	Small Grains
Maximum water uptake w_{up}^* [cm]	63	68.48	40
Maximum nitrogen uptake n_{up}^* [kgN/ha]	300	187.50	250
Salinity critical value $\overline{EC}$ [dS/m]	30	53.85	85

*Data source: Maas and Hoffman (1977), Pang and Letey (1998), and Crohn et al. (2009).

Table 3: Corn relative yield function

Function		Estimated Parameters					Ψ
		1	s	s^2	s^3	R^2	R^2
	b_w^1	1.8143E-02	-7.0787E-04	1.4785E-05	-6.5115E-08	0.9973	
	b_w^0	-1.0316E+01	-2.4081E-01	-2.6960E-02	8.0481E-04	0.9815	
	b_n^1	9.3959E-02	2.1530E-01	-1.5375E-02	2.9392E-04	0.7995	
Relative Yield $(ry)^\dagger$	b_n^0	2.3456E-04	-4.9809E-05	2.9616E-06	-5.2352E-08	0.9524	0.9973
[-]	d_0	-2.1708E+00	3.9813E-02	3.7506E-03	-1.8434E-04	0.7736	
	d_1	6.2726E-02	1.3402E-04	-2.6225E-05	5.0871E-06	0.9846	
	d_2	2.9870E-01	4.9733E-03	-1.3716E-03	2.3810E-05	0.9993	

† Relative yield function: $\Psi_{ry}\left(w,n,s\right) = \left(1-\exp\left(-b_w^1(s)\left(\varphi(w)\ w - b_w^0(s)\right)\right)\right)\left(1-\exp\left(-b_n^1(s)\left(n-b_n^0(s)\right)\right)\right)$
where $\varphi\left(w\right) = \frac{4\exp(d_1(s)w+d_0(s))}{(1+\exp(d_1(s)w+d_0(s)))^2} + d_2(s)$

Table 4: Corn water uptake function

Function		Estimated Parameters					Ψ
		1	s	s^2	s^3	R^2	R^2
	b_w^1	1.8525E-02	-7.8960E-04	1.9666E-05	-1.5166E-07	0.9977	
	b_w^0	-1.0092E+01	-2.9076E-01	-2.3904E-02	7.4959E-04	0.9816	
	b_n^1	1.2619E+01	-1.0002E+00	5.6978E-02	-1.1916E-03	0.7032	
Water Uptake (w_{up})†	b_n^0	-8.3833E+00	-8.5954E-01	4.4055E-02	-3.6489E-04	0.5158	0.9973
[cm]	d_0	-2.3167E+00	7.0209E-02	1.9723E-03	-1.5336E-04	0.8084	
	d_1	6.4865E-02	-3.0723E-04	-7.3700E-07	4.6484E-06	0.9854	
	d_2	2.9041E-01	6.7238E-03	-1.4749E-03	2.5620E-05	0.9990	

† Water uptake function: $\Psi_{w_{up}}(w,n,s) = \left(1-\exp\left(-b_w^1(s)\left(\varphi(w)\ w - b_w^0(s)\right)\right)\right)\left(1-\exp\left(-b_n^1(s)\left(n-b_n^0(s)\right)\right)\right)$
where $\varphi(w) = \frac{4\exp(d_1(s)w+d_0(s))}{(1+\exp(d_1(s)w+d_0(s)))^2} + d_2(s)$

Table 5: Corn nitrogen uptake function

Function		Estimated Parameters					Ψ
		1	s	s^2	s^3	R^2	R^2
Nitrogen Uptake (n_{up})† [kg/ha]	b_w^1	4.1660E-02	-6.2435E-04	1.9684E-04	-2.6517E-06	0.9989	0.9956
	b_w^0	-3.8416E+01	3.8479E-01	6.0445E-02	-1.4881E-03	0.9992	
	b_n^1	7.9577E-03	1.6436E-05	-2.6500E-06	4.6767E-08	0.9961	
	b_n^0	-1.1849E+00	-7.2459E-03	1.4038E-03	-3.1992E-05	0.8800	
	d_0	-1.0656E+00	-2.8598E-02	5.4957E-03	-1.1587E-04	0.9941	
	d_1	5.2347E-02	7.3267E-04	-4.7909E-05	1.3255E-06	0.9778	
	d_2	2.8552E-03	6.0586E-04	-1.1421E-04	2.9139E-06	0.7705	

† Nitrogen uptake function: $\Psi_{n_{up}}(w,n,s) = (1-\exp(-b_w^1(s)(\varphi(w)\ w - b_w^0(s))))(1-\exp(-b_n^1(s)(n-b_n^0(s))))$
where $\varphi(w) = \frac{4\exp(d_1(s)w+d_0(s))}{(1+\exp(d_1(s)w+d_0(s)))^2} + d_2(s)$

Table 6: Corn nitrate leaching function

Function		Estimated Parameters				Ψ
		1	s	s^2	R^2	R^2
	ϑ_w^1	4.1465E-01	-2.3226E-02	4.0842E-04	0.9067	
Nitrate Leaching $(nl)^{\S}$	ϑ_w^0	8.8139E+01	4.5549E-03	-8.7404E-03	0.9734	0.9734
[kg/ha]	ϑ_n	8.8789E-02	6.6406E-03	-6.8241E-05	0.9878	

§ Nitrate leaching function: $\Psi_{nl}(w,n,s) = (\vartheta_n(s) \cdot n)\left(1 + \exp\left(-\vartheta_w^1(s)\left(w - \vartheta_w^0(s)\right)\right)\right)^{-1}$

Table 7: Cotton response functions

Functions		Estimated Parameters						Ψ
		1	s	s^2	s^3	$\sqrt{s}$	R^2	R^2
Water Uptake (w_{up})† [cm]	b_w^1	2.4758E-02	-5.5610E-02	4.6684E-04	–	2.3827E-01	0.9983	0.9850
	b_w^0	2.9370E+00	3.7825E-01	-3.8065E-03	–	-1.7042E+00	0.9672	
	b_n^1	3.4761E-02	-9.5432E-04	9.7281E-06	–	3.3671E-03	0.9865	
	b_n^0	-1.0048E+03	-6.9806E+01	4.3059E-01	–	4.4738E+02	0.9913	
	d_0	-1.9310E-01	-4.8508E-01	3.6268E-03	–	2.4483E+00	0.9997	
	d_1	3.0048E-02	1.3073E-03	1.6158E-05	–	-7.4888E-03	0.9932	
	d_2	2.2604E-01	2.3395E-02	-1.7739E-04	–	-1.3251E-01	0.9749	
Nitrogen Uptake (n_{up})‡ [kg/ha]	b_w^1	4.1347E-02	-9.5788E-04	1.3248E-04	-2.0094E-06	–	0.7922	0.9301
	b_w^0	-8.1342E+01	3.5931E+01	-1.1290E+00	8.4346E-03	–	0.9218	
	b_n^1	1.0014E-02	8.4480E-05	-1.5166E-05	2.5512E-07	–	0.9233	
	b_n^0	-5.7776E-02	-4.0057E-02	-4.5261E-02	9.4218E-04	–	0.8831	
	d_0	-2.7723E+00	7.0878E-01	-2.5691E-02	2.3649E-04	–	0.9786	
	d_1	2.3927E-02	1.4263E-02	-6.7201E-04	7.7165E-06	–	0.7584	
	d_2	3.1032E+00	-2.2247E+00	1.4816E-01	-1.9775E-03	–	0.9799	
Relative Yield (ry)‡ [-]	b_w^1	4.2910E-02	4.1989E-02	-7.8219E-04	–	–	0.9969	0.9135
	b_w^0	4.5197E+00	9.8234E-02	–	–	-1.3980E+00	0.9924	
	b_n^1	2.8070E-02	2.1351E-03	-2.6165E-06	–	–	0.9586	
	b_n^0	4.1684E-02	8.3436E-04	–	–	-1.2605E-02	0.9749	
	d_0	4.3794E-01	2.8471E-01	-5.2277E-03	–	–	0.9618	
	d_1	2.7633E-02	-7.8865E-04	3.8162E-05	–	–	0.9992	
	d_2	4.0487E-01	6.4077E-03	–	–	-1.0180E-01	0.9909	
Nitrate Leaching (nl)§ [kg/ha]	ϑ_w^1	1.2103E-01	-1.6859E-03	8.7523E-06	–	–	0.9285	0.9932
	ϑ_w^0	1.0767E+02	-1.3533E-01	-5.5516E-03	–	–	0.9966	
	ϑ_n	2.4911E-01	3.7287E-03	-1.1199E-05	–	–	0.9510	

† Water uptake function: $\Psi(w,n,s) = (1-\exp(-b_w^1(s)(\varphi(w)\ w - b_w^0(s))))(1-\exp(-b_n^1(s)(n-b_n^0(s))))$ where $\varphi(w) = \frac{4\exp(d_1(s)w+d_0(s))}{(1+\exp(d_1(s)w+d_0(s)))^2} + d_2(s)$

‡ Nitrogen uptake function or relative yield function: $\Psi(w,n,s) = (1-\exp(-b_w^1(s)(\varphi(w)\ w - b_w^0(s))))(1-\exp(-b_n^1(s)(n-b_n^0(s))))$ where $\varphi(w) = \frac{4\exp(d_1(s)w+d_0(s))}{(1+\exp(d_1(s)w+d_0(s)))^2} + (d_2(s))^2$

§ Nitrate leaching function: $\Psi_{nl}(w,n,s) = (\vartheta_n(s)\cdot n)(1+\exp(-\vartheta_w^1(s)(w-\vartheta_w^0(s))))^{-1}$

Table 8: Small Grains response functions

Functions		Estimated Parameters						Ψ
		1	s	s^2	s^3	$\sqrt{s}$	R^2	R^2
Water Uptake (w_{up})† [cm]	b_w^1	5.4887E-02	8.8365E-04	–	–	-1.2660E-02	0.9992	0.9895
	b_w^0	-1.4706E+00	3.8352E-01	–	–	-4.6480E+00	0.9995	
	b_n^1	3.3459E-02	3.6858E-04	–	–	-5.2111E-03	0.9887	
	b_n^0	-1.0577E+03	2.2656E+01	–	–	-3.2040E+02	0.9999	
	d_0	-1.1065E+01	-1.7822E-01	–	–	2.6840E+00	0.9995	
	d_1	2.3098E-01	4.9613E-03	–	–	-5.5987E-02	0.9969	
	d_2	7.3158E-01	-2.3317E-02	–	–	1.2677E-01	0.9699	
Nitrogen Uptake (n_{up})† [kg/ha]	b_w^1	2.3093E-02	1.0020E-03	-5.4338E-05	8.2254E-07	–	0.9937	0.9760
	b_w^0	-2.7373E+01	3.0280E-01	2.4283E-02	-2.8201E-04	–	0.9995	
	b_n^1	7.5630E-03	-1.4065E-04	2.6628E-06	-1.1513E-08	–	0.9914	
	b_n^0	3.5255E+00	-9.6064E-01	2.2256E-02	-1.0843E-04	–	0.9979	
	d_0	3.4820E+00	-5.9384E+00	2.4480E-01	-2.0653E-03	–	0.9677	
	d_1	-7.8489E-02	8.8699E-03	-4.2253E-03	4.8533E-05	–	0.9799	
	d_2	6.9359E-01	8.8347E-02	8.0244E-04	-2.2655E-05	–	0.9995	
Relative Yield (ry)† [-]	b_w^1	2.1015E-02	-3.7979E-04	3.1736E-06	–	–	0.9999	0.9920
	b_w^0	-9.7590E+00	-2.4221E-01	2.5489E-03	–	–	0.9990	
	b_n^1	1.7967E-02	-8.0471E-04	6.1540E-05	–	–	0.9997	
	b_n^0	6.9662E-02	-2.6187E-03	2.1165E-05	–	–	0.9899	
	d_0	-3.3623E+00	8.7670E-02	-7.6724E-04	–	–	0.9931	
	d_1	8.8470E-02	-1.4634E-03	2.3777E-05	–	–	0.9945	
	d_2	9.4826E-01	-1.4023E-02	2.2275E-05	–	–	0.9918	
Nitrate Leaching (nl)§ [kg/ha]	ϑ_w^1	7.2178E-01	8.0706E-03	–	–	-1.2705E-01	0.9987	0.9732
	ϑ_w^0	8.1202E+01	-2.8048E-01	–	–	6.7213E-01	0.8654	
	ϑ_n	2.8377E-02	1.8152E-03	–	–	-5.6472E-03	0.9998	

† Water uptake function, nitrogen uptake function, or relative yield function: $\Psi\left(w,n,s\right) = \left(1-\exp\left(-b_w^1(s)\left(\varphi(w)\ w-b_w^0(s)\right)\right)\right)\left(1-\exp\left(-b_n^1(s)\left(n-b_n^0(s)\right)\right)\right)$ where $\varphi\left(w\right)=\frac{4\exp(d_1(s)w+d_0(s))}{(1+\exp(d_1(s)w+d_0(s)))^2}+d_2(s)$

§ Nitrate leaching function: $\Psi_{nl}\left(w,n,s\right)=\left(\vartheta_n(s)\cdot n\right)\left(1+\exp\left(-\vartheta_w^1(s)\left(w-\vartheta_w^0(s)\right)\right)\right)^{-1}$

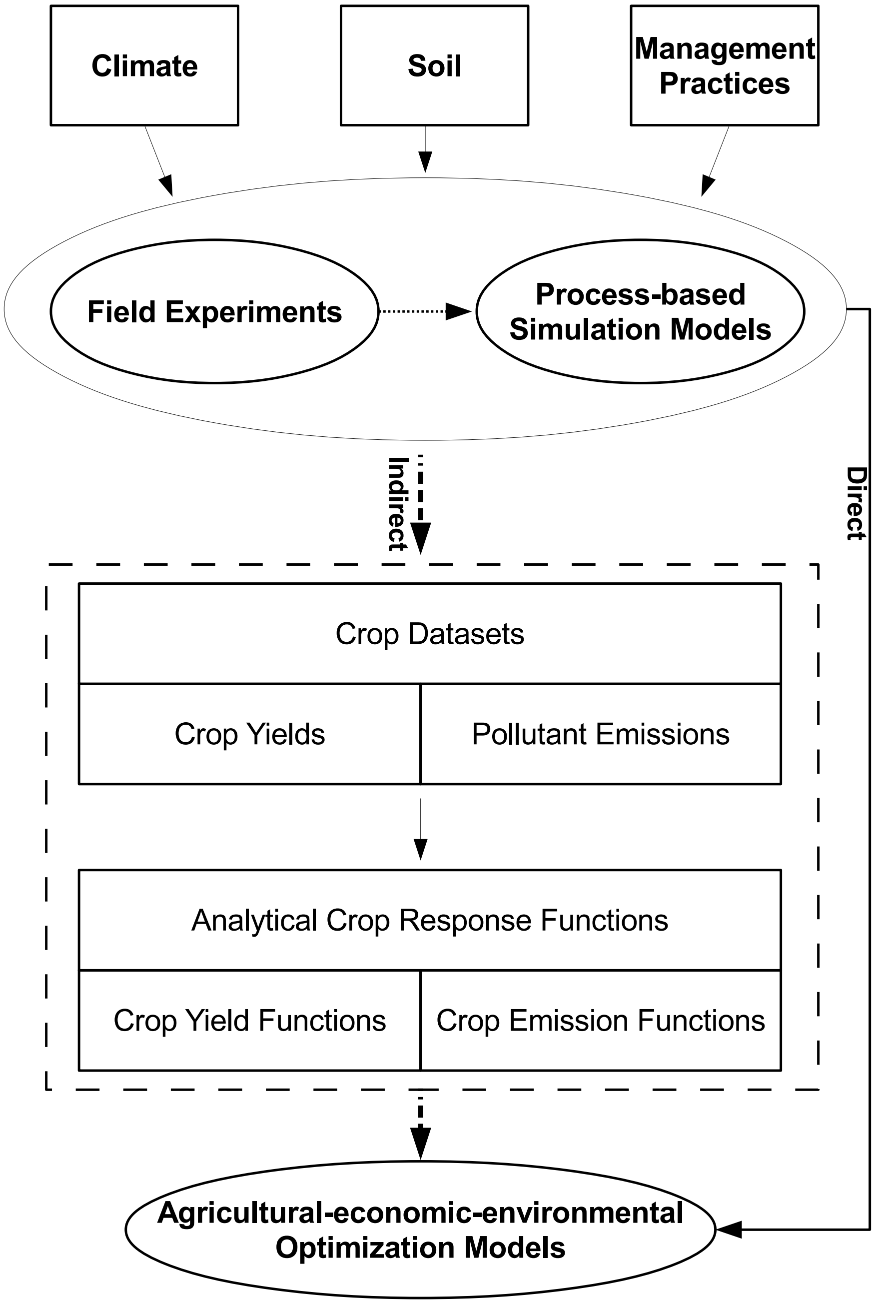

Figure 1: Alternative approaches for linking process-based simulation models with optimization models

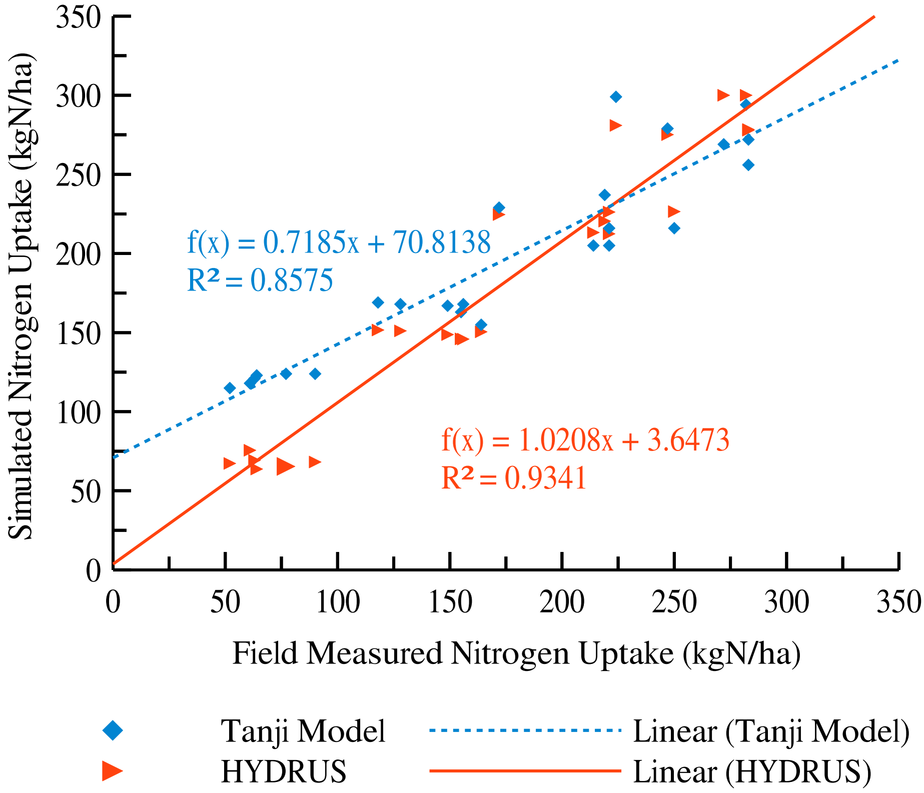

Figure 2: Field measured nitrogen uptake vs. simulated nitrogen uptake from Tanji et al. (1979) model & from HYDRUS-1D

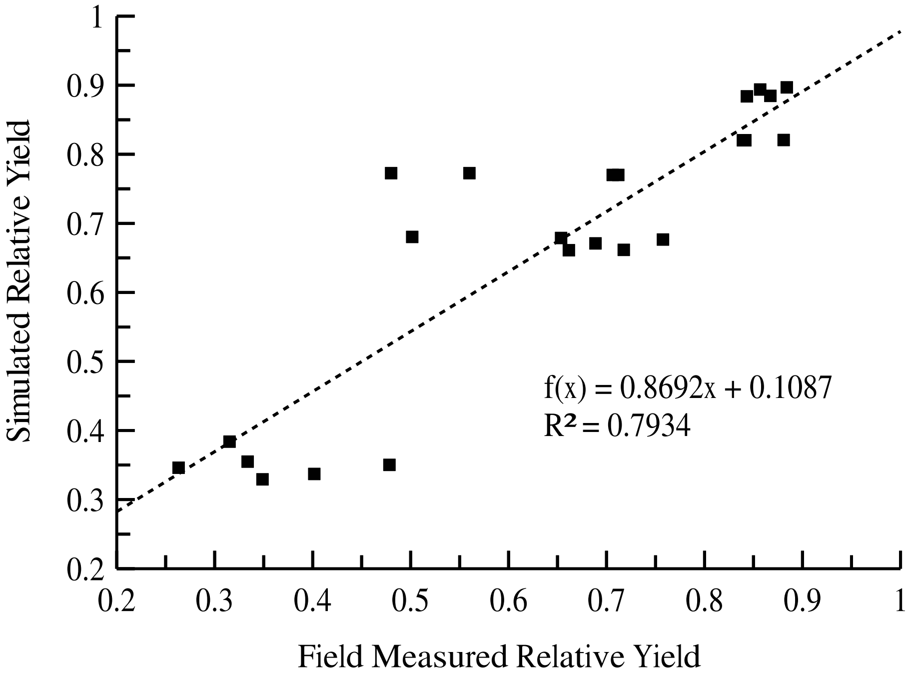

Figure 3: Field measured relative yield vs. simulated relative yield from our model

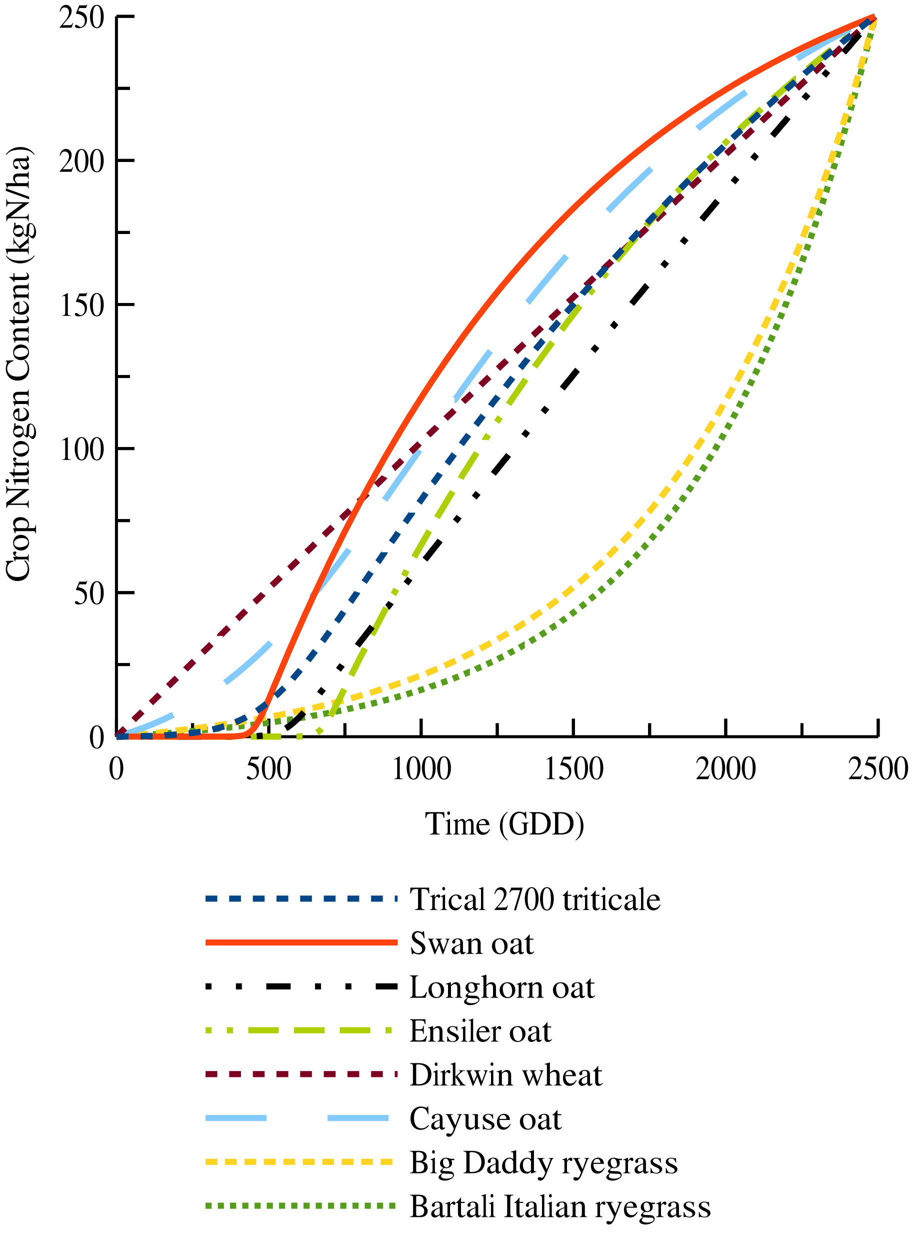

Figure 4: Nitrogen uptake curves for eight small grain forages commonly grown in California. Source: Crohn et al. (2009).

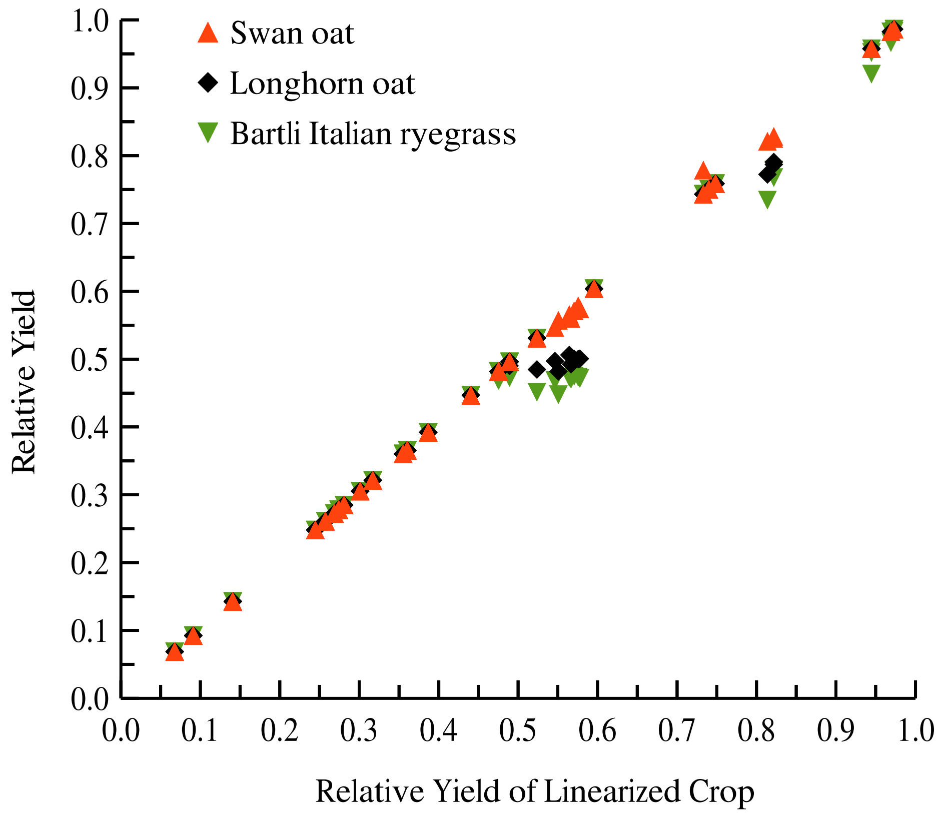

Figure 5: Relative yield of the linearized crop vs. relative yield of Swan oat, Longhorn oat, and Bartali Italian ryegrass

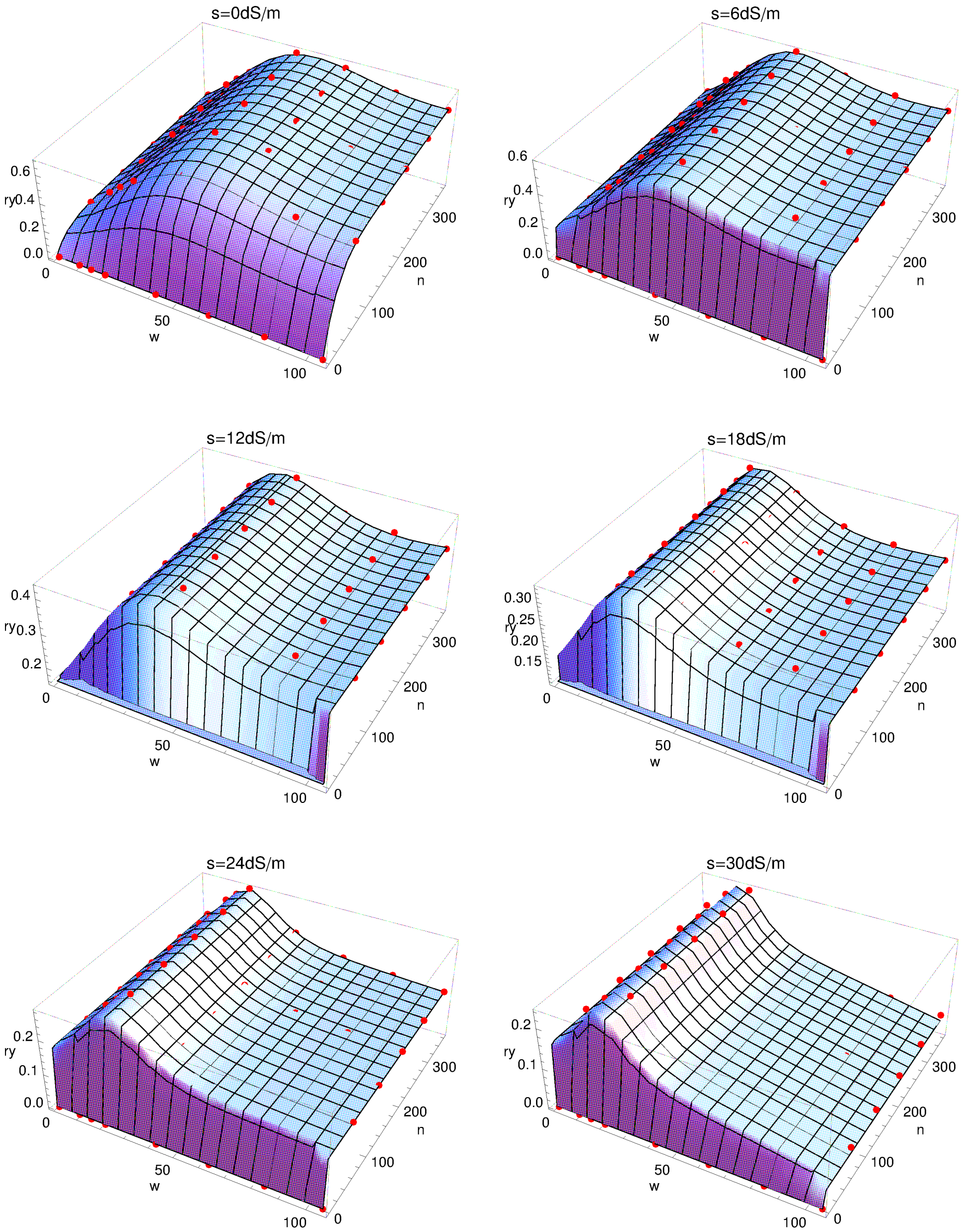

Figure 6: Relative yield vs. available water and available nitrogen for corn when soil salinity is $0, 6, 12, 18, 24$, and $30\,\mathrm{dS/m}$. Points: simulated data. Surfaces: fitted functions.

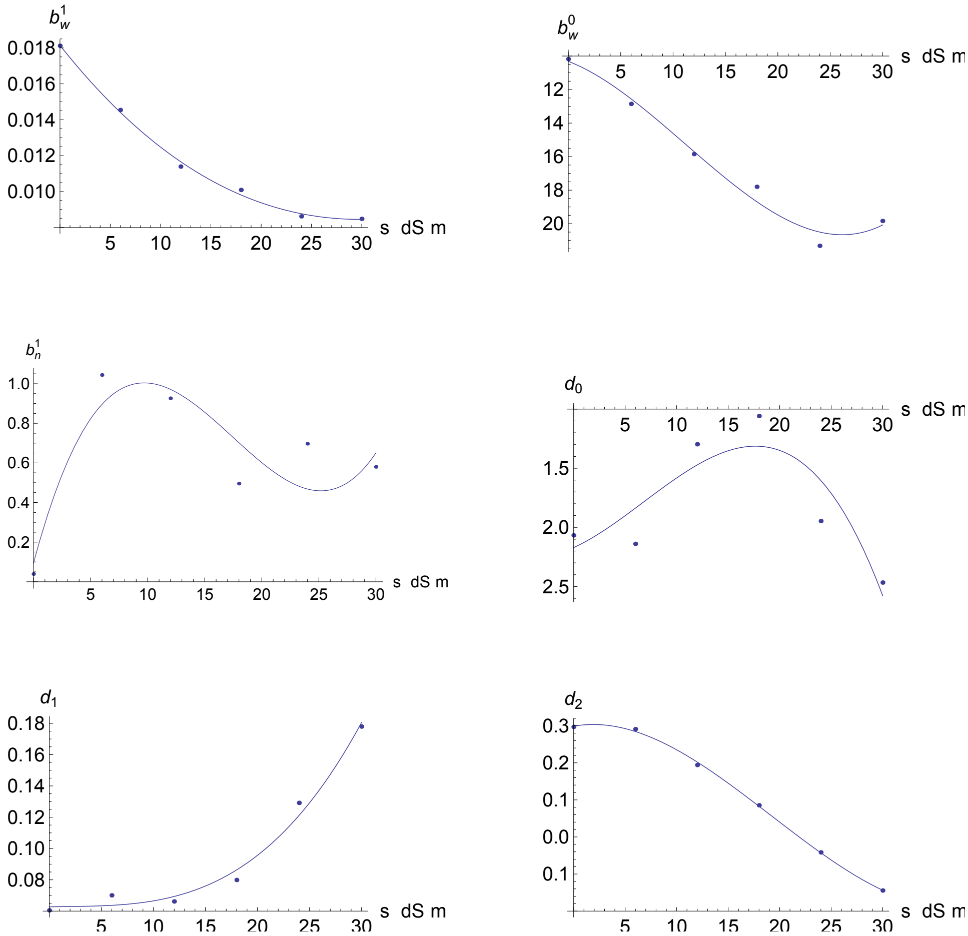

Figure 7: Polynomial regression of water and nitrogen parameters in the relative yield function for corn

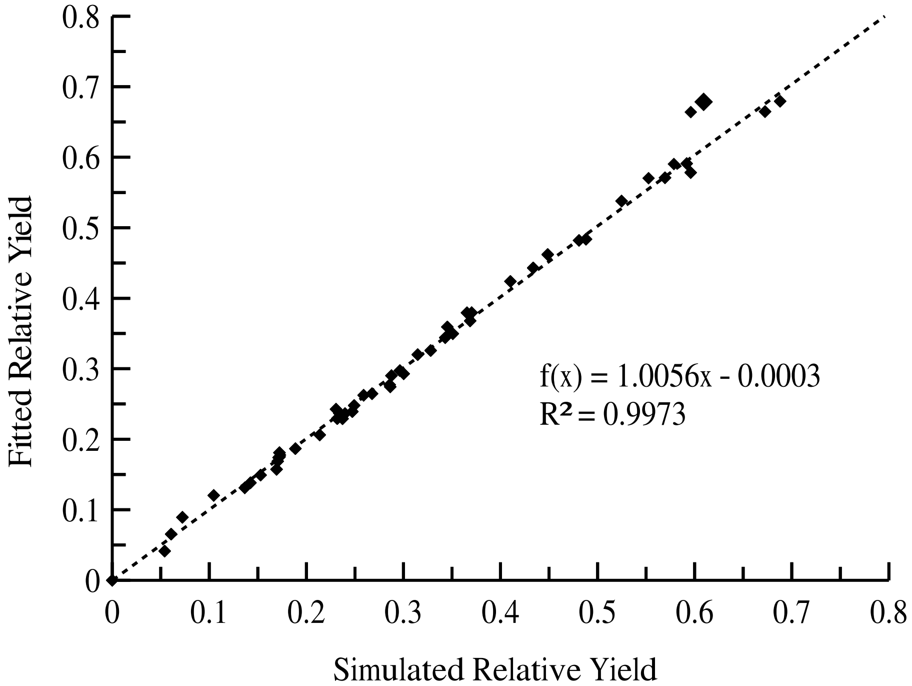

Figure 8: Relative yield function for corn: simulated data vs. fitted data

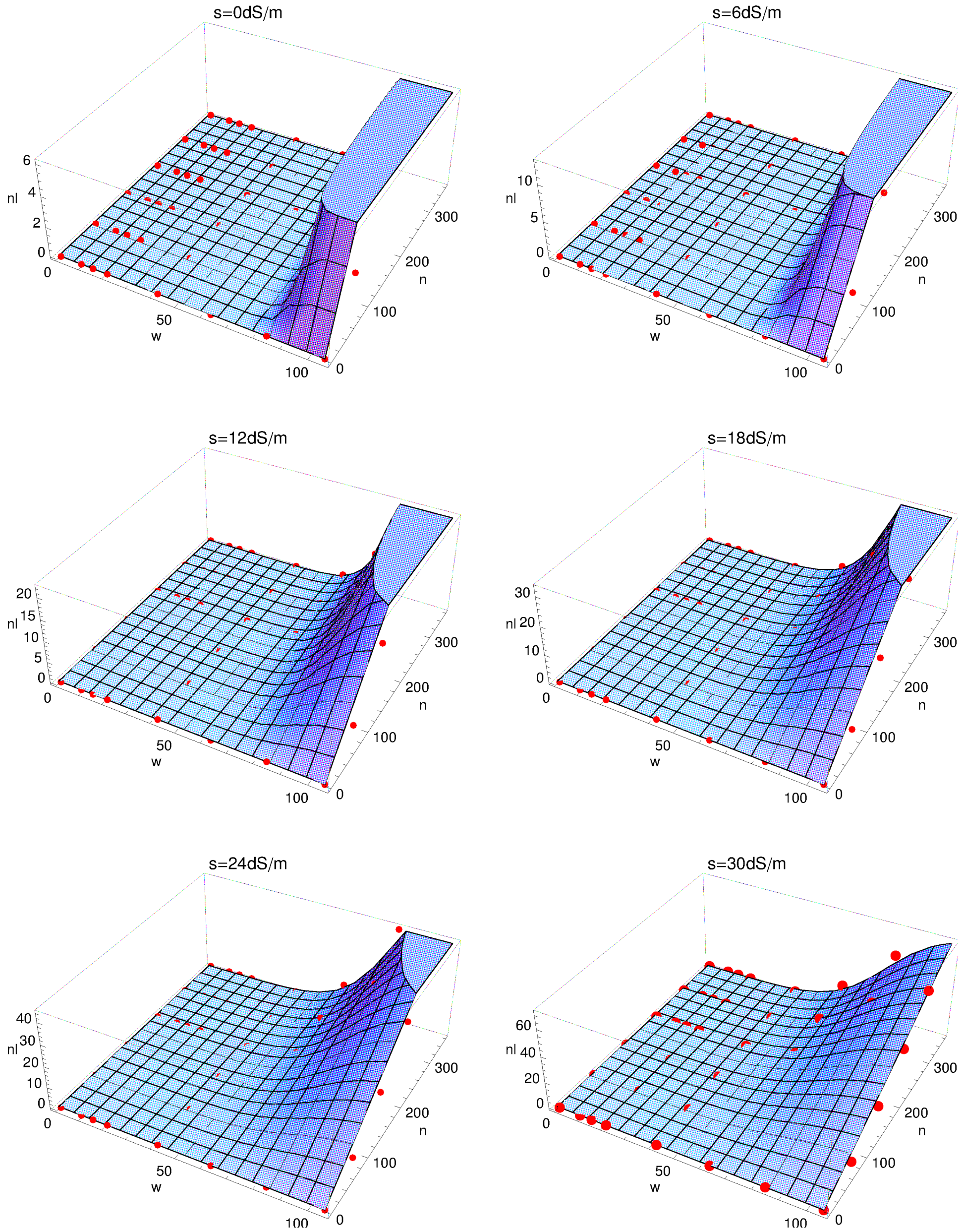

Figure 9: Nitrate leaching vs. available water and available nitrogen for corn when soil salinity is 0, 6, 12, 18, 24,and 30 dS/m. Points: simulated data. Surfaces: fitted functions.

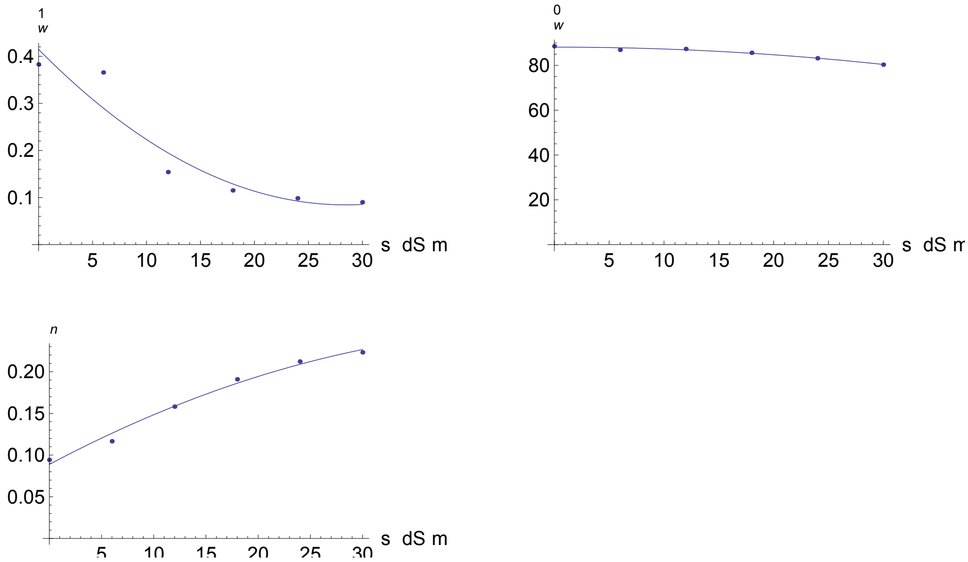

Figure 10: Polynomial regression of water and nitrogen parameters in the nitrate leaching function for corn

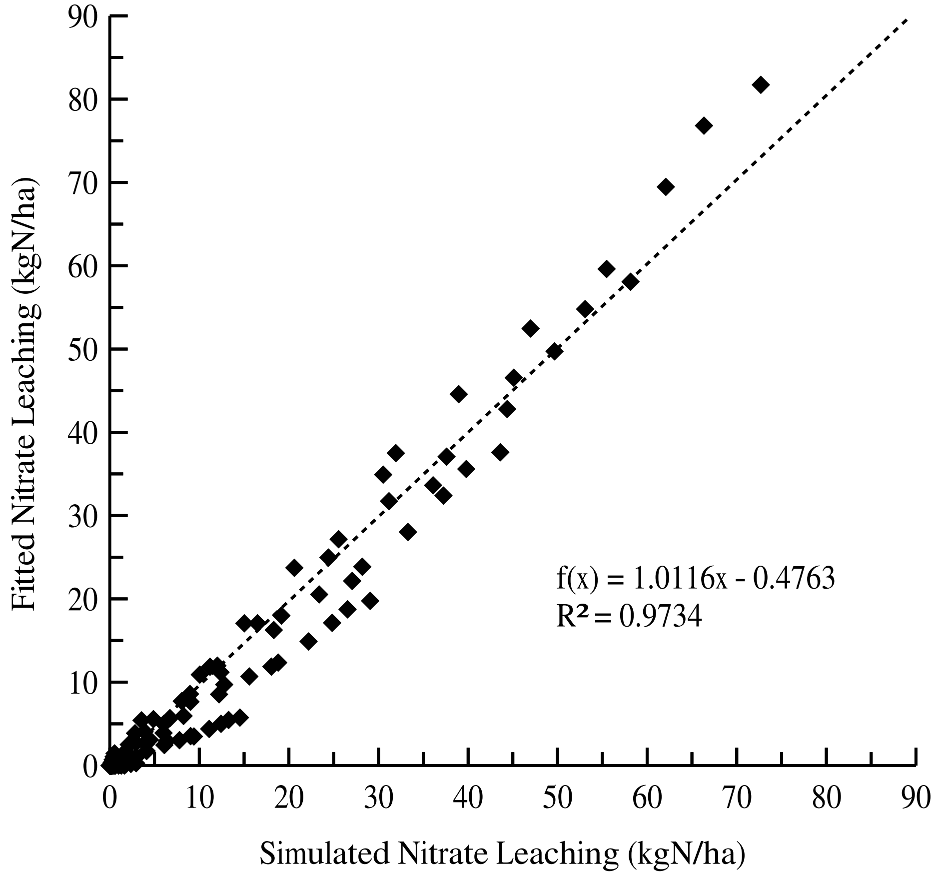

Figure 11: Nitrate leaching function for corn: fitted data vs. simulated data

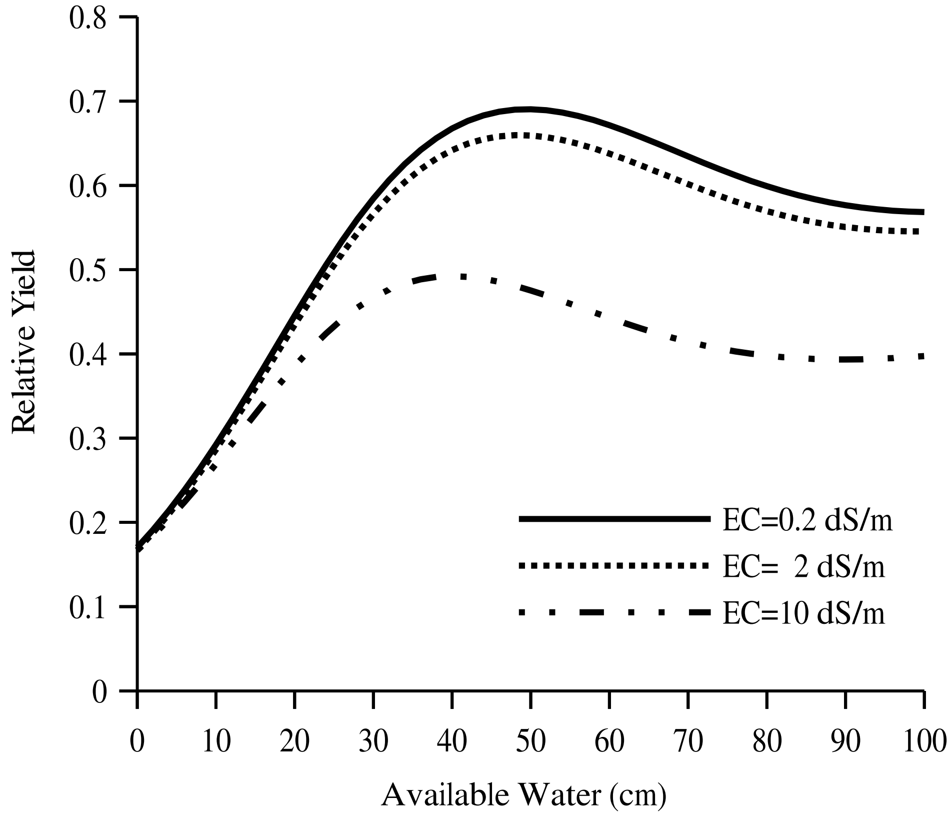

Figure 12: Interactions of water, nitrogen, and salinity for corn relative yield

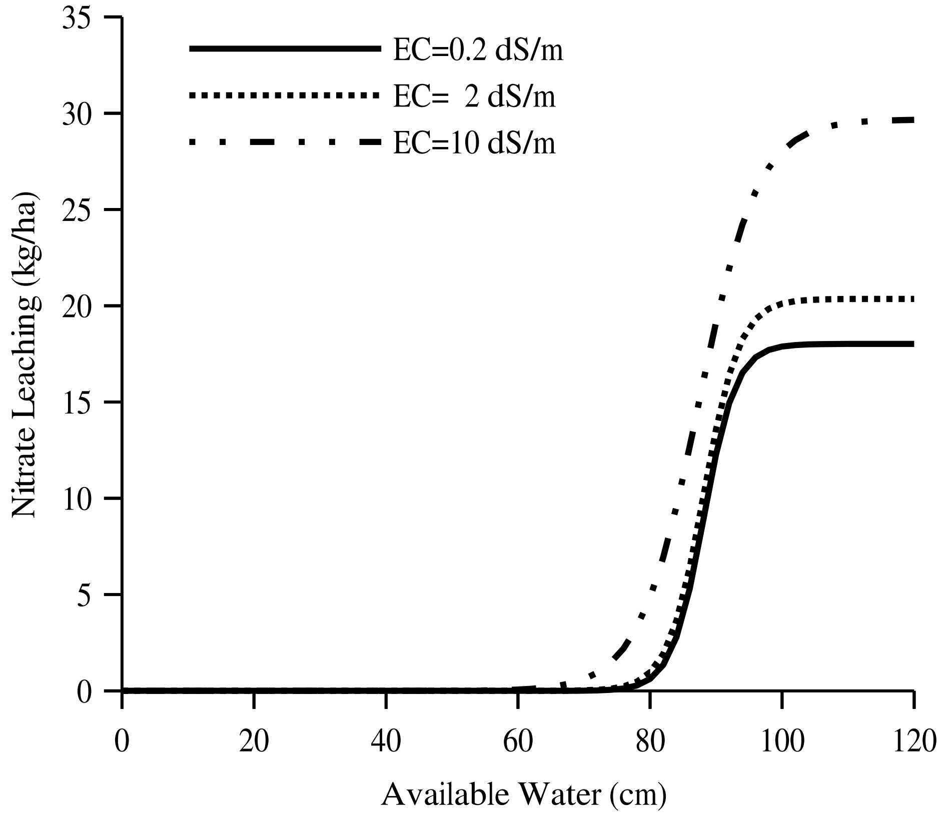

Figure 13: Interactions of water, nitrogen, and salinity for corn nitrate leaching